Modelling NO2 concentrations at the street level in the GAINS integrated assessment model: projections under current legislation

G. Kiesewetter, J. Borken-Kleefeld, W. Schopp, C. Heyes, P. Thunis, Bertrand Bessagnet, Etienne Terrenoire, A. Gsella, Markus Amann

Atmos. Chem. Phys., 14, 813–829, 2014
www.atmos-chem-phys.net/14/813/2014/
doi:10.5194/acp-14-813-2014

Atmospheric Chemistry and Physics
Open Access

Modelling NO_2 concentrations at the street level in the GAINS integrated assessment model: projections under current legislation

G. Kiesewetter[1], J. Borken-Kleefeld[1], W. Schöpp[1], C. Heyes[1], P. Thunis[2], B. Bessagnet[3], E. Terrenoire[3], A. Gsella[4], and M. Amann[1]

[1]International Institute for Applied Systems Analysis (IIASA), Schlossplatz 1, 2361 Laxenburg, Austria
[2]Joint Research Centre, Institute for Environment and Sustainability (JRC-IES), Ispra, Italy
[3]National Institute for Environment and Risks (INERIS), Paris, France
[4]European Environment Agency, Copenhagen, Denmark

Correspondence to: G. Kiesewetter (kiesewet@iiasa.ac.at)

Received: 1 August 2013 – Published in Atmos. Chem. Phys. Discuss.: 30 August 2013
Revised: 4 December 2013 – Accepted: 9 December 2013 – Published: 24 January 2014

Abstract. NO_2 concentrations at the street level are a major concern for urban air quality in Europe and have been regulated under the EU Thematic Strategy on Air Pollution. Despite the legal requirements, limit values are exceeded at many monitoring stations with little or no improvement in recent years. In order to assess the effects of future emission control regulations on roadside NO_2 concentrations, a downscaling module has been implemented in the GAINS integrated assessment model. The module follows a hybrid approach based on atmospheric dispersion calculations and observations from the AirBase European air quality database that are used to estimate site-specific parameters. Pollutant concentrations at every monitoring site with sufficient data coverage are disaggregated into contributions from regional background, urban increment, and local roadside increment. The future evolution of each contribution is assessed with a model of the appropriate scale: 28×28 km grid based on the EMEP Model for the regional background, 7×7 km urban increment based on the CHIMERE Chemistry Transport Model, and a chemical box model for the roadside increment. Thus, different emission scenarios and control options for long-range transport as well as regional and local emissions can be analysed. Observed concentrations and historical trends are well captured, in particular the differing NO_2 and total $NO_x = NO + NO_2$ trends. Altogether, more than 1950 air quality monitoring stations in the EU are covered by the model, including more than 400 traffic stations and 70 % of the critical stations. Together with its well-established bottom-up emission and dispersion calculation scheme, GAINS is thus able to bridge the scales from European-wide policies to impacts in street canyons. As an application of the model, we assess the evolution of attainment of NO_2 limit values under current legislation until 2030. Strong improvements are expected with the introduction of the Euro 6 emission standard for light duty vehicles; however, for some major European cities, further measures may be required, in particular if aiming to achieve compliance at an earlier time.

1 Introduction

NO_2 is a traffic-related air pollutant that is of major concern for public health, both through direct effects and as a precursor to tropospheric ozone formation (WHO, 2006). For the European Union (EU), legally binding limit values on NO_2 concentrations have been defined in the Air Quality Directive (EU, 2008) and its Daughter Directives. Member States are facing considerable difficulties to meet these limit values, with 22 out of 27 Member States still recording exceedances as of 2010 (EEA, 2012). In spite of the past reductions in emissions of total nitrogen oxides ($NO_x = NO + NO_2$), NO_2 concentrations at roadside stations have shown only small decreases or even increases during recent years, which has been attributed to increasing shares of primary NO_2 in emissions from diesel cars (Carslaw, 2005).

The GAINS Integrated Assessment Model[1] (Amann et al., 2011) is employed in the current revision of the EU Thematic Strategy on Air Pollution (TSAP) as a policy analysis tool to provide an outlook on the likely development of air quality under different emission control strategies, and assess their costs and benefits. The GAINS model brings together information on the sources and impacts of air pollutant and greenhouse gas emissions and their interactions. GAINS addresses air pollution impacts on human health and ecosystems, in addition to the mitigation of greenhouse gas emissions. As an input to the revision of the TSAP, the impact of different emission scenarios on compliance with air quality limit values is assessed. GAINS air quality impact calculations are currently done on a resolution of roughly 7×7 km for human health. This resolution is sufficient to describe urban background conditions; compliance with air quality limit values, however, is determined at single monitoring stations which may be located in street canyons at traffic hot spots and therefore require a significantly finer model resolution.

Modelling pollution levels inside street canyons with heavy traffic is challenging, owing mostly to the physical description of the air flow and the quantification of emissions, whereas the chemical processes are relatively well understood. Detailed models have shown impressive results in describing pollution levels within street canyons (for an overview see e.g. Vardoulakis et al., 2003), attempting to explicitly model the air flow through computational fluid dynamics (Sabatino et al., 2007; Murena et al., 2009) or introducing a parametrisation of turbulence (Berkowicz, 2000). Owing to the complexity of input information required, models used in these studies are often limited to single cities or even single street canyons (Denby, 2011). The focus of the GAINS model, however, is to provide estimates for the evolution of air quality and compliance with limit values in the EU as a whole. This results in the need to model concentrations in the immediate vicinity of hundreds of traffic stations. It is infeasible to gather sufficient data to employ detailed street canyon models for all these stations. We therefore base our modelling scheme on a combination of bottom-up modelling and past observations, employing the chemical description used in parametrised models such as OSPM (Berkowicz, 2000) but estimating physical input parameters from past observations.

In this article, we describe the downscaling scheme that has been implemented in the GAINS model to assess compliance with limit values at individual monitoring stations reporting to the European air quality database (AirBase)[2]. Starting from monitoring data, we disaggregate measured annual mean concentrations at roadside monitoring sites into the appropriate measured background and a local traffic increment. We then attempt to explain both contributions to the extent possible with the available models and relate them to the relevant emission sources; unexplained residuals are kept constant. The same scheme is applied for stations classified as background or industrial stations, however without calculation of a roadside increment.

With this modelling scheme, GAINS is able to estimate NO_2 concentrations for more than 1950 monitoring stations, more than 400 of which are traffic stations, including a large fraction of the currently exceeding stations. Scenario calculations until 2030 have been provided as an input to the revision of the TSAP (Amann et al., 2013). As an application of the modelling scheme, we here discuss the projected evolution of compliance with NO_2 limit values under current legislation.

The remainder of this article is organised as follows. Section 2 provides a detailed description of the modelling scheme. Section 3 presents a validation of modelled concentrations against past observations. Necessary simplifications contained in the modelling scheme lead to station-specific uncertainties and limitations of the model, which are discussed in Sect. 4. In Sect. 5, the evolution of NO_2 concentrations under current legislation is assessed. Section 6 presents a summary and draws conclusions.

2 Modelling scheme

2.1 Overview

The EU air quality legislation specifies two different limit values for NO_2 concentrations: a limit of $40\,\mu g\,m^{-3}$ on annual mean concentrations, and a limit value of $200\,\mu g\,m^{-3}$ on hourly mean concentrations, not to be exceeded more than 18 times per calendar year. Our modelling scheme is designed to calculate annual mean concentrations and thus cannot directly provide estimates on compliance with the limit value on hourly mean concentrations. However, in practice the annual mean limit value presents a significantly more stringent target than the hourly limit value: in 2009, all but five stations complying with the annual mean limit value also complied with the hourly limit value. The same pattern is confirmed throughout previous observational years. Therefore, although we focus only on annual means, conclusions are also possible about compliance with the hourly limit value.

The modelling scheme combines past monitoring data with bottom-up emission modelling. The starting point of all calculations is monitoring data reported to AirBase in 2009. To ensure quality of the data, we consider only stations with more than 80 % temporal coverage of the hourly data. AirBase comprised more than 2500 NO_2 monitoring stations in the EU in 2009, with a substantial subset of these monitoring data also used to determine compliance with limit values.

A schematic overview of the modelling scheme is shown in Fig. 1. For any roadside monitoring station that fulfils the 80 % data coverage requirement, observed concentrations (left blue bar) are first disaggregated into an appropriate

[1] Greenhouse gas – Air pollution INteractions and Synergies, online at http://gains.iiasa.ac.at.

[2] http://acm.eionet.europa.eu/databases/airbase/

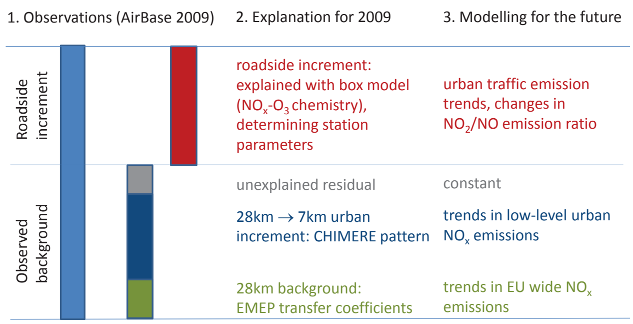

Fig. 1. Schematic overview of the traffic station scheme. Observed roadside concentrations (left) are first disaggregated into background and traffic increment (step 1), then the different components are explained to the extent possible for 2009 (step 2). For the roadside increment, this involves estimating the station-specific parameters (residence time of air in the street canyon, background representativeness correction if needed). For the modelling of scenario years other than the base year (step 3), we consider changes in European-wide NO_x emissions for the background, and changes in urban driving emissions (including changes in primary NO_2 emissions) for the traffic increment.

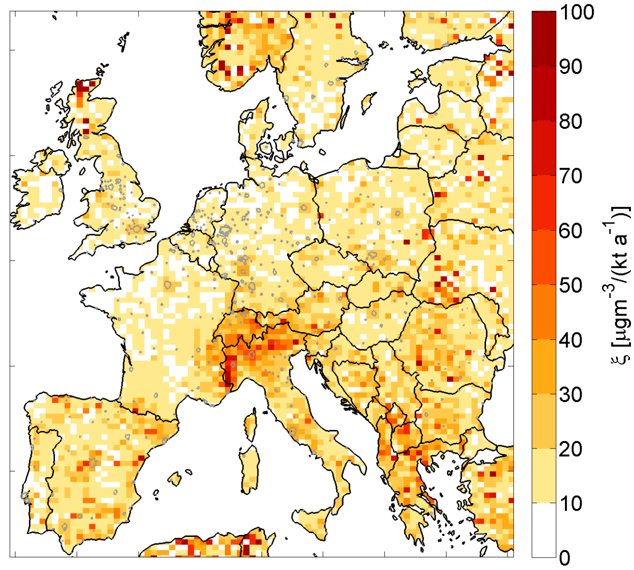

Fig. 2. Regression coefficient ξ relating NO_x emissions to concentration increments in CHIMERE.

observed background[3] and the roadside increment. This first step of disaggregation is essential, since the two contributions have different sources and hence need to be modelled independently. For a station labelled as background station in AirBase, no disaggregation of the observed concentration is undertaken.

As a second step, we attempt to explain the two contributions with the model and relate them to the relevant emissions. Background concentrations are calculated as a regional scale background and an urban scale increment, as described in detail in Sect. 2.2. The residual from calculated to observed background concentrations constitutes an unexplained part that is kept constant for scenario applications. The roadside increment is calculated with a simple parametrised box model, detailed in Sect. 2.3.

In the third step, the application to future emission scenarios, we modify each component following the change in related emissions, using the parameters determined in step two (see Sect. 2.4).

2.2 Modelling background concentrations

By definition, background concentrations at a roadside station are made up from all contributions other than local traffic in the street where the station is located. This encompasses large-scale transboundary transport of pollution, but also an urban background increment caused by low-level emissions from within the rest of the city.

Due to the short chemical lifetime of NO_2, it is advantageous to treat NO_2 as a member of the reactive nitrogen (NO_x) family. All bottom-up background calculations described in this chapter are done for NO_x, and only in a final step is the partitioning into NO_2 and NO calculated.

NO_x concentrations resulting from emissions in the entire EU are modelled in GAINS based on linear transfer coefficients calculated with the EMEP MSC-W Chemical Transport Model (CTM; Simpson et al., 2012) at a resolution of 0.5° (lon) × 0.25°(lat) or roughly 28 × 28 km; see Sect. 2.2.1 for further details. To capture sub-28 km structures, we use a full year simulation performed with the CHIMERE CTM (Menut et al., 2013; Schmidt et al., 2001; Vautard et al., 2005; Bessagnet et al., 2008) at a resolution of 0.125° × 0.0625°or roughly 7 × 7 km. The CHIMERE grid is nested in the EMEP grid, so that 4 × 4 CHIMERE grid cells match exactly one EMEP grid cell.

Both models use the same spatial disaggregation of emissions, which has been generated specifically for this work, as detailed in Appendix A.

The spatial domain of the CHIMERE model, which is also the domain considered in the station modelling scheme as a whole, can be seen in Fig. 2.

The different steps of the background modelling are discussed in detail in the following subsections.

2.2.1 The 28 × 28 km background: EMEP

The EMEP sensitivity simulations use meteorological fields of the years 2006, 2007, 2008, 2009, and 2010, and the emissions expected in the year 2020. In each sensitivity run, NO_x

[3] The "appropriate background" is determined as the mean of all background stations with the same type of area classification and the same city name (if available), or within a 20 km radius otherwise. If no such stations are available, stations with a "lower" classification of area type are taken into account, e.g. suburban background stations for an urban traffic station.

emissions from one source region were reduced by 15 %, allowing the change in concentrations at each grid point to be related to the change in emissions. In total, 53 source regions were included: EU-28, Switzerland, Norway, Iceland, Serbia and Montenegro, Belarus, Bosnia-Herzegovina, Turkey, Ukraine, Moldova, FYR Macedonia, Georgia, Armenia, Albania, Azerbaijan, Russia (European part), and 10 sea regions as defined by Campling et al. (2013).

The NO_x transfer coefficient $\nu(\boldsymbol{i}, r)$ from source region r to receptor grid cell $\boldsymbol{i} = \begin{pmatrix} i_{\mathrm{lon}} \\ i_{\mathrm{lat}} \end{pmatrix}$ is defined as

$$\nu(\boldsymbol{i}, r) = \frac{[\mathrm{NO_x}]_{\mathrm{base}}(\boldsymbol{i}) - [\mathrm{NO_x}]_{\mathrm{red}}(\boldsymbol{i})}{0.15 E_{\mathrm{base}}(r)}, \tag{1}$$

with $[\mathrm{NO_x}]$ denoting the annual mean NO_x concentration in grid cell $\boldsymbol{i}$, $E(r)$ the annual total NO_x emissions from source region r, and the labels base and red referring to the base case (full emissions) and the reduced emission model run.

From the transfer coefficients, concentrations $[\mathrm{NO_x}](\mathbf{i})$ are calculated as

$$[\mathrm{NO_x}](\boldsymbol{i}) = \delta(\boldsymbol{i}) + \sum_{r=1}^{n_r} E(r) \cdot \nu(\boldsymbol{i}, r). \tag{2}$$

The constant $\delta(\boldsymbol{i})$ quantifies the residual NO_x concentration emerging from hemispheric background, natural sources and non-linearities in the system. It is calculated by inserting the base case emissions and concentrations in Eq. (2),

$$\delta(\boldsymbol{i}) = [\mathrm{NO_x}]_{\mathrm{base}}(\boldsymbol{i}) - \sum_{r=1}^{n_r} E_{\mathrm{base}}(r) \cdot \nu(\boldsymbol{i}, r). \tag{3}$$

For most European regions, this residual is less than $\pm 10\,\%$ of base case modelled NO_x, with maxima of $-20\,\%$ or around $-3\,\mu\mathrm{g\,m^{-3}}$ in the Po valley.

2.2.2 Downscaling to 7 × 7 km: CHIMERE

We employ the CHIMERE CTM at a resolution of $0.125° \times 0.0625°$ using meteorological fields and emissions for 2009. Significant modifications have been included in the CHIMERE code to ensure optimal simulation of urban conditions: WRF 3-D meteorological variables were substituted by ECMWF-IFS data, to avoid overestimation of wind speed and thus too fast dispersion of emissions within urban areas (Miglietta et al., 2012). Furthermore, to account for the urban canopy influence on meteorology, wind speed and vertical diffusion (K_z coefficient) were modified empirically. In the lowest model layer, the wind speed was multiplied by a factor 0.5, in accordance with Solazzo et al. (2009), who found in a computational fluid dynamics study that the wind speed in the urban canopy layer is roughly half of that in the undisturbed boundary layer.

In the CTM output, a robust linear relation exists between the low-level NO_x emissions and concentration increments. Let $\boldsymbol{m} = \begin{pmatrix} m_{\mathrm{lon}} \\ m_{\mathrm{lat}} \end{pmatrix}$ identify a 7 km CHIMERE grid cell and $\boldsymbol{i}(\boldsymbol{m})$ identify the 28 km EMEP grid cell that contains $\boldsymbol{m}$. Higher-than-average NO_x low-level emission density e_{L} in sub-grid $\boldsymbol{m}(\boldsymbol{i})$ leads to a corresponding increase in ground level NO_x concentrations above the EMEP grid average, and vice versa for negative deviations. We can find a regression coefficient $\xi(\boldsymbol{i})$ linking concentration increments to emissions so that

$$[\mathrm{NO_x}](\boldsymbol{m}) = [\mathrm{NO_x}](\boldsymbol{i}(\boldsymbol{m})) + \xi(\boldsymbol{i}(\boldsymbol{m})) \cdot \{e_{\mathrm{L}}(\boldsymbol{m}) - e_{\mathrm{L}}(\boldsymbol{i}(\boldsymbol{m}))\}. \tag{4}$$

Here $e_{\mathrm{L}}(\boldsymbol{i}(\boldsymbol{m}))$ denotes the average low-level emission density in the 28 km grid, calculated by averaging the 7 km emission densities $e_{\mathrm{L}}(\boldsymbol{m})$ over the respective 28 km grid $\boldsymbol{i}$. e_{L} contains all sources of emissions that are released into the lowest vertical layer of CHIMERE: domestic, road traffic, and non-road traffic emissions (in the SNAP nomenclature[4], sectors 2, 7, and 8). ξ is calculated for every EMEP grid cell by regressing emission increments $e_{\mathrm{L}}(\boldsymbol{m}) - e_{\mathrm{L}}(\boldsymbol{i}(\boldsymbol{m}))$ against concentration increments $[\mathrm{NO_x}](\boldsymbol{m}) - [\mathrm{NO_x}](\boldsymbol{i}(\boldsymbol{m}))$ and contains all local meteorological characteristics. A map of ξ for the whole domain is shown in Fig. 2. The impact on concentrations of a single additional ton of pollutant being emitted in a grid cell differs significantly throughout Europe, owing to the different meteorological conditions. For example, frequent stagnant conditions lead to higher values of ξ in the Alps and the Po valley than in northern Europe.

Since this resolution-dependent concentration increment is relevant mostly in urban areas, we refer to it also as urban increment, although it is calculated for every EMEP grid cell regardless of its location. EMEP grid cells containing parts of the same urban area are combined in the regression analysis, thus enhancing the statistical significance of the calculation. Each major city is thus assigned a single characteristic value of ξ. Two examples of the data behind the ξ calculation in European cities are shown in Fig. 3: Paris (top panel) and Milan (bottom panel). Although both cities show a compact linear correlation between emissions and their concentration effects, the slopes (ξ values) differ by a factor of two. Similarly high R^2 values are found throughout most of Europe, in particular in urban areas where emission and concentration increments are high.

The modelled 7 × 7 km concentration given by Eq. (4) has a tendency to underestimate observed urban background concentrations in medium-sized and smaller cities. This is at least partly related to the fact that 7 km is still rather large for smaller cities, which do not fill entire grid cells, especially if they are distributed over several grid cells. Thus we undertake a further disaggregation of emissions into urban and suburban parts of a given CHIMERE grid cell $\boldsymbol{m}$, which is described further in Sect. 2.2.3.

[4]Selected Nomenclature for Air Pollution, see e.g. EEA (2007).

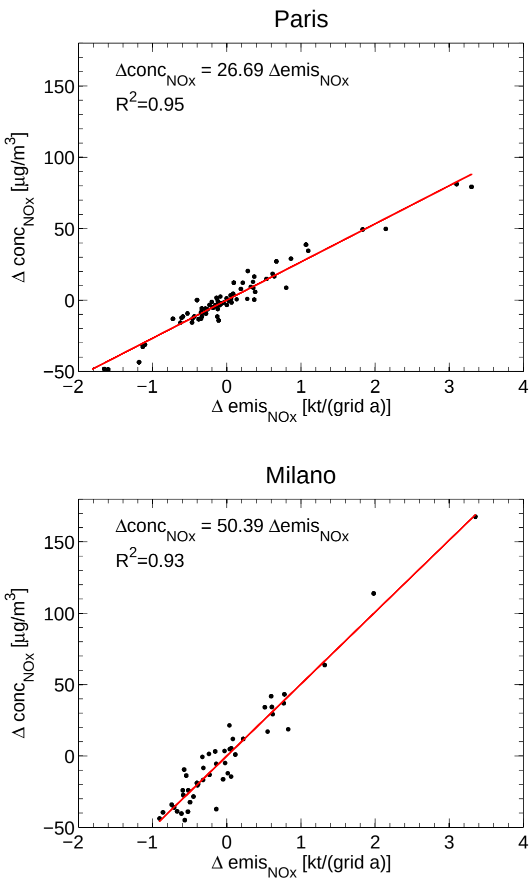

Fig. 3. NO_x emission vs. concentration increments in the CHIMERE model run around two major European cities: Paris (top panel) and Milan (bottom panel). Each dot represents a grid cell. All EMEP grid cells which contain parts of the urban area are combined here. The linear fit is shown as a red line. Note the different slopes of the fit, corresponding to the different meteorological characteristics of these cities.

2.2.3 Further disaggregation: inner-urban concentrations

Structures smaller than the 7 km CHIMERE grid are not reflected in the emission inventory nor in the model output. Many emissions, however, scale with population density, which is available at a much finer resolution. Here we have used population density on a resolution of roughly 1×1 km (Gallego, 2010) to determine urban polygon shapes for European cities with a population $> 100\,000$, as detailed in Appendix B. These polygons are used to split CHIMERE grid cells partly containing urban areas into an urban part (red in Fig. 4) and a suburban part (yellow in Fig. 4). Emissions from the domestic sector and from all traffic sources except heavy duty trucks are redistributed according to population numbers inside and outside the urban polygon, so that for these sectors, s, the inner urban emission density, e_u, from

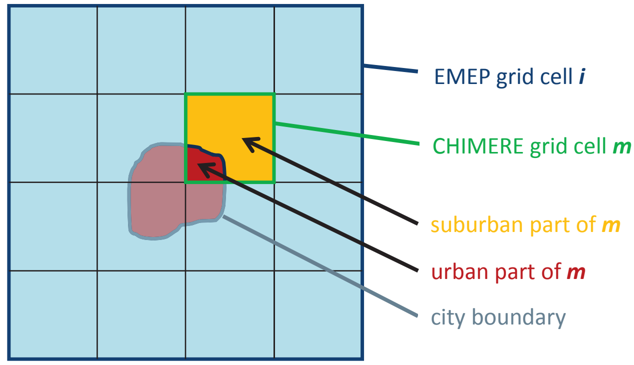

Fig. 4. Disaggregation of CHIMERE grid cell $\boldsymbol{m}$ into urban (red) and suburban (yellow) parts.

region r in $\boldsymbol{m}$ is then given by

$$e_u(\boldsymbol{m},r,s) = e(\boldsymbol{m},r,s)\,\frac{\mathrm{pop_u}(\boldsymbol{m})}{\mathrm{pop_{tot}}(\boldsymbol{m})}\,\frac{A_{tot}(\boldsymbol{m})}{A_u(\boldsymbol{m})}, \tag{5}$$

with $\mathrm{pop_u}$ and A_u representing population and area inside the urban polygon, $\mathrm{pop_{tot}}$ and A_{tot} those of the entire grid cell. NO_x concentrations inside the urban polygon are calculated from Eq. (4) using the inner urban emission density e_u instead of the 7 km grid average e. Outside the urban polygon, emission densities are lowered from the grid average by the equivalent factor.

Whether the urban or the suburban concentration is taken as representative for the background of a given traffic station (or the modelled concentration at a background station) depends entirely on the location of the station inside or outside the urban polygon.

The background calculation scheme detailed in Sects. 2.2.1–2.2.3 is used to calculate NO_x concentrations. In a final step, NO_2 concentrations are calculated from NO_x by applying the modelled NO_2/NO_x concentration ratio from the 2009 CHIMERE simulation in each grid cell individually.

2.3 Modelling the roadside increment

For traffic stations, the local roadside increment is calculated with a simple parametrised box model that considers NO_x–O_3 photochemistry and mixing with the background. The chemical core has been described by Palmgren et al. (1996) and Düring et al. (2011) and is also used in the OSPM parametrised street pollution model (Berkowicz, 2000).

The model calculates steady-state NO_2 concentrations in the street canyon from roadside NO_x concentrations, the share of NO_2 in local NO_x road traffic emissions, concentrations of NO_2, NO_x, and O_3 in the urban background, and the characteristic mixing time of air in the street canyon.

The mixing time of air is a station-specific characteristic, depending on the layout of buildings around the station, typical wind speeds etc. Since these data are not readily available for all traffic stations in AirBase, we estimate the mixing time from past observations. Details on the traffic increment model formulation are given in Sect. 2.3.1. The Monte Carlo-based parameter estimation process is described in Sect. 2.3.2.

2.3.1 The parametrised model

A detailed description of the steady-state model is given by Düring et al. (2011). Only NO oxidation by O_3 and NO_2 photolysis are considered, as all other reactions involving NO_x happen on timescales distinctly longer than the typical residence times of air in the street canyon (around 40–100 s). The chemical equations involved are

$$NO_2 + h\nu \xrightarrow{J} NO + O \tag{6}$$

$$O + O_2 + M \rightarrow O_3 + M \tag{7}$$

$$NO + O_3 \xrightarrow{k} NO_2 + O_2, \tag{8}$$

with k and J the reaction constants for NO_2 formation and photolysis, respectively.

Under the influence of NO and NO_2 emissions on the one hand and mixing with the background on the other hand, steady-state roadside NO_2 concentrations are given by (Düring et al., 2011)

$$[NO_2]_{ss} = 0.5 \cdot \left\{ B - \sqrt{B^2 - 4\left([NO_x][NO_2]_O + \frac{[NO_2]_n}{k\tau}\right)} \right\} \tag{9}$$

with

$$[NO_2]_n = [NO_2]_V + [NO_2]_B$$
$$[NO_2]_O = [NO_2]_n + [O_3]_B$$
$$B = [NO_x] + [NO_2]_O + \frac{1}{k}\left(J + \frac{1}{\tau}\right)$$
$$[NO_2]_V = p\left([NO_x] - [NO_x]_B\right).$$

The following quantities are used:

$[NO_x]$	roadside NO_x = NO + NO_2 concentration
$[NO_2]_B$	NO_2 background concentration
$[NO_x]_B$	NO_x background concentration
$[O_3]_B$	O_3 background concentration
τ	typical residence time of air in the street canyon
k	reaction constant for Eq. (8)
J	photolysis reaction constant (Eq. 6)
p	share of NO_2 in NO_x traffic emissions in the street

Düring et al. (2011) use this model to explain annual mean observed roadside NO_2 concentrations from annual mean observed background concentrations and externally determined mixing time τ. Here we use Eq. (9) first to estimate τ from observational data in 2009 (see Sect. 2.3.2), and then apply it to scenario calculations (see Sect. 2.4), starting from modelled background concentrations.

2.3.2 Estimation of site-specific parameters

In Eq. (9), a traffic station is characterised by a single parameter, the characteristic residence time of air in the street canyon (τ). If all other quantities entering the calculation are known from observations, it is possible to invert Eq. (9) and calculate τ. However, in doing so, all uncertainty is concentrated in this one parameter. Reasonable ranges for τ are known to be between 40–100 s (Düring et al., 2011). For several traffic stations, direct inversion of Eq. (9) gives physically meaningless values far outside this range or even below zero.

Parts of the difficulties here are connected to uncertainties in the other input quantities, in particular the measured background concentrations. There are good arguments for different ways of calculating an appropriate background concentration from observations (see Sect. 2 above for details on the methodology applied here), but none can be truly representative for the background air above the roof level close to the traffic station with which the air in the street canyon is mixed: by definition, background stations are typically located somewhat remotely from busy roads. Even within one city, observed urban background concentrations of NO_2 and NO_x vary strongly (Cyrys et al., 2012). It is thus reasonable to assume that the observed city average background may not be fully representative of the local background concentrations entering Eq. (9) – in some cases, a representativeness correction is needed. This is designed here as a relative correction in order to make it easily transferable to future scenario years in which the mean value may have changed substantially:

$$[NO_x]_B = \widetilde{[NO_x]}_B \cdot (1 + \lambda_{NO_x}\sigma_{NO_x}) \tag{10}$$

$$[NO_2]_B = \widetilde{[NO_2]}_B \cdot (1 + \lambda_{NO_x}\sigma_{NO_2}) \tag{11}$$

$$[O_3]_B = \widetilde{[O_3]}_B \cdot (1 + \lambda_{O_3}\sigma_{O_3}). \tag{12}$$

The same parameter λ_{NO_x} is used in Eqs. (10) and (11) to ensure consistency between NO_2 and NO_x background representativeness corrections. σ_{NO_x}, σ_{NO_2}, and σ_{O_3} are the average relative standard deviations of NO_x, NO_2 and O_3 background monitoring stations, averaged over all European cities with more than two background stations operational in 2009. $\widetilde{[NO_x]}_B$, $\widetilde{[NO_2]}_B$, and $\widetilde{[O_3]}_B$ are observed background values. We also recognise that the NO_2 emission share p is not known exactly for a given station, but do not include it in our analysis, as a relative correction cannot be easily transferred to the future (p is determined by the technology mix which changes over time).

With the above parameters, we reformulate the problem of characterising a traffic station as an estimation problem: given the measured value of NO_2, and the measured (or modelled, in the case of p) input quantities, what are the most likely values for the parameters τ, λ_{NO_x}, and λ_{O_3}?

Estimation theory provides several solution pathways for such a problem. Most analytical ones, however, require the

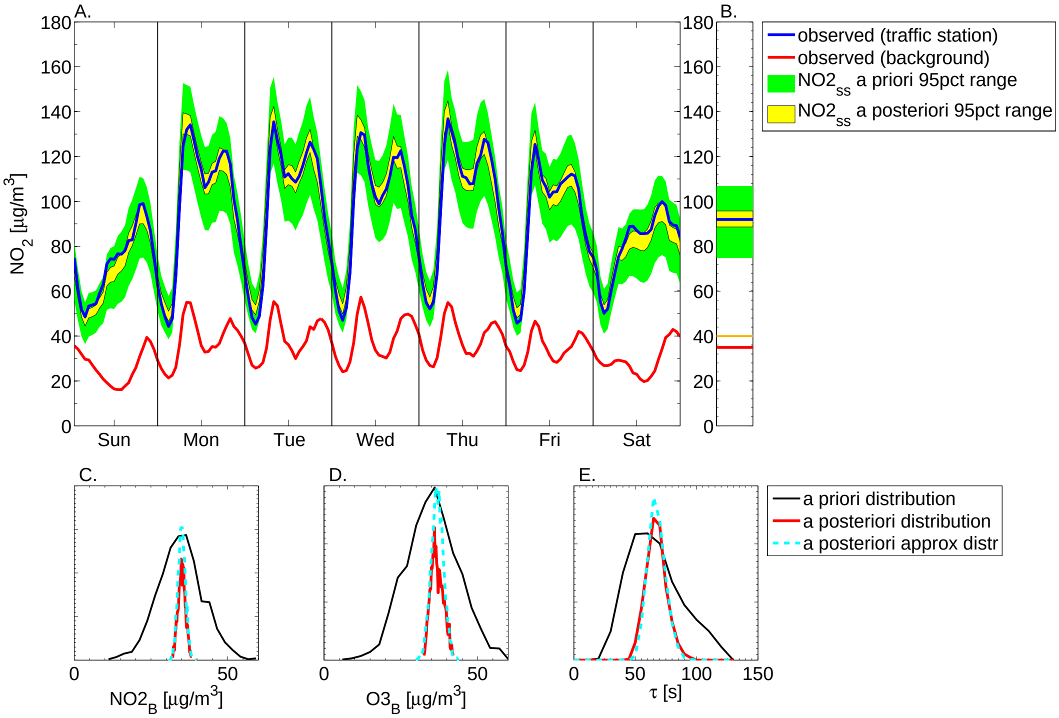

Fig. 5. Parameter estimation from the annual average weekly pattern of observations at Landshuter Allee traffic station, Munich. **(A)** Weekly pattern of observed roadside (blue) and background (red) NO_2 concentrations in 2009, the 95 percentile range of explained concentrations with a priori input parameter distributions (green area), and the 95 percentile range of concentrations modelled with a posteriori parameter distributions after the estimation process (yellow). **(B)** Average of concentrations shown in **(A)** over all hours of the week, corresponding to the annual average. **(C–E)** Distributions of involved input quantities before (black) and after (red) the parameter estimation, and the approximation of the latter by normal (log-normal in the case of τ) distributions (cyan, dashed). For ease of viewing, distributions in **(C–E)** are not normalised.

model equation to be linear in its parameters, which is not the case with Eq. (9).

We solve the estimation problem by minimising a penalty function through Monte Carlo simulation, similar to the approach described by Dilks et al. (1992). For this purpose, we assign distributions to the parameters: λ_{NO_x} and λ_{O_3} are assumed to follow a standard linear distribution (mean = 0, variance = 1), while τ is assumed to be log-normally distributed with median and width approximately as given in the literature: $\tilde{\tau} = 70$ s and $\sigma_\tau = 30$ s. The log-normal distribution is chosen mainly to strictly avoid negative numbers of τ. The parameters are assumed to be uncorrelated.

Mathematically, we seek to estimate parameters from the a priori information supplied in the input distributions. Equation (9) is strongly under-determined if three parameters are inserted: from just one observed variable, annual mean $[NO_2]$, it is impossible to extract enough information to estimate three parameters – in this case, the solution would depend strongly on the assumed a priori distributions.

A way forward is to exploit more of the actual information available from AirBase and apply Eq. (9) not to annual mean, but to hourly values. Theoretically, up to $365 \times 24 = 8760$ measurement points are available for each station in the base year. However, the time series is dominated by short-term fluctuations in turbulent mixing conditions and emissions, which are not represented in the simple model formulation. To eliminate the noise from short-term meteorology, we consider the annual average *weekly pattern* instead, in which the time series has been averaged according to the hour of the week (see Fig. 5a). Thus we effectively use $24 \times 7 = 168$ data points for the estimation process, thereby turning the under-determined equation into an over-determined system of 168 equations with three unknowns.

For the estimation process, we acknowledge that also observed roadside $\widetilde{[NO_2]}$ is not known perfectly well but subject to some (observational) uncertainty. Effectively, we search for a solution to Eq. (9) which matches observed $\widetilde{[NO_2]}$ as well as necessary (to stay within the limits of observational accuracy), while altering input parameters as little as possible from their a priori values. For this purpose, we introduce a penalty function that weights residuals in calculated steady-state $[NO_2]_{ss}$ against departures of input parameters from their expected values:

$$f = |\lambda_{NO_x}| + |\lambda_{O_3}| + |\lambda_\tau| + \left| \frac{[NO_2]_{ss}(\lambda_{NO_x}, \lambda_{O_3}, \lambda_\tau) - \widetilde{[NO_2]}}{\sigma_{obs}} \right|. \quad (13)$$

σ_{obs} represents the acceptable deviation between model and observation, which is empirically set to 1 % of the observed concentration.

The solution is found by minimising f. Since the calculation is performed for every hour of the week, we minimise the sum of f calculated for every hour. We perform a Monte Carlo simulation, drawing for each parameter a large number of samples ($n = 100\,000$). The best 1 % of solutions then make up the a posteriori distributions, which can be quite well approximated as Gaussian distributions (see Fig. 5c–e). Their mean values are taken as the solution, while the width of the distributions may be used in an uncertainty analysis. The aim here is to determine a robust solution; we do not necessarily require the solution to be optimal in the sense of estimation theory.

An example for the parameter estimation is shown in Fig. 5 for the Landshuter Allee traffic station, a monitoring station located at a busy road in Munich. The observed weekly pattern of roadside NO_2 (panel a), showing the characteristic fingerprint of a traffic station, is well reproduced by the model; however, the explained concentration range is large if the whole a priori range of parameters is considered (green area). The estimation process narrows the relatively broad a priori distributions of parameters (black lines in panels c–e) to the most likely values (red lines in c–e), resulting in the a posteriori range of modelled NO_2 concentrations (yellow area in a).

The parameters determined in this step are meant to give a simple representation of the station characteristics. They are calculated for the year 2009 and are assumed to remain unchanged in the past and the future.

2.4 Combining background and roadside increment models

On the European average, NO_2 at urban traffic stations is made up of roughly equal contributions from urban background and roadside increment in the base year. In individual countries, this allocation varies between 40 % and 70 %. The roadside increment itself is composed of roughly 50 % primary emitted NO_2 and 50 % oxidised NO emissions. This apportionment into "primary" and "secondary" NO_2 varies between different countries, depending on the country-specific value of p determined by the fleet mix (particularly the share of diesel vehicles).

Once the different contributions from regional background, urban increment, and traffic increment have been established from observations for the base year 2009, and the station-specific parameters have been determined from Monte Carlo-based estimation, the model is ready for scenario analysis. Essentially, this means replacing the emissions for 2009 with emissions for the desired scenario year.

We do not model urban background O_3 trends but assume O_3 levels to remain constant at 2009 observed levels. For modelled NO_2 and NO_x background concentrations, a simple calibration to the observed values in 2009 is done: if the model under-estimates observations in the base year, the offset is regarded as missing sources (unexplained fraction) and kept constant for other years. On the other hand, if the model over-predicts observed background concentrations in 2009, modelled concentrations are scaled by the ratio of observed/modelled concentrations in the base year. This calibration is motivated by the need for background concentrations to be consistent with observations in 2009 as the roadside increment model is calibrated to the observed background. Although the distinction into positive and negative offsets is artificial, it ensures that model predictions in a future with declining emissions are always on the conservative, i.e. pessimistic, side.

The NO_2/NO_x partitioning ratio used to derive urban background NO_2 concentrations from urban background NO_x is kept constant for the future, in accordance with the assumption that urban background O_3 levels remain unchanged. A discussion on the possible limitations of this approach is given in Sect. 4.

The formulation of the traffic increment model implies that knowledge of the exact amount of traffic emissions generated in the individual street canyon is not necessary. Instead, roadside NO_x concentrations are needed. Since NO_x is chemically inert at timescales of seconds to minutes, we calculate roadside NO_x concentrations in any scenario year y by scaling the observed increment in the base year y_0 with the trend in road traffic emissions,

$$\frac{[NO_x](y) - [NO_x]_B(y)}{[NO_x](y_0) - [NO_x]_B(y_0)} = \frac{E_{road}(y)}{E_{road}(y_0)}. \tag{14}$$

2.4.1 Emission calculation

Emissions are calculated in the GAINS model bottom-up from a given projection of activity (fuel consumption), accounting for fleet turnover and penetration of vehicles with different stages of emission controls. We calculate emissions for countries (using national emission factors), and for average urban conditions in each country.

Vehicle fleets are known to differ in composition in urban areas from the national average (Carslaw et al., 2011b): the share of heavy trucks is much lower in urban driving than nationally, yet there are more buses and motorised two-wheelers. To account for these general differences we determined for each vehicle category its share of distance driven in urban areas, based on model estimates from COPERT (Ntziachristos et al., 2009) or national inventories where available (Carslaw et al., 2011a; Knoerr et al., 2012). Also unit emissions differ in urban areas from the country average: in particular for heavy duty vehicles it is known that NO_x exhaust after-treatment has not functioned well at urban speeds, and hence unit emissions are several times higher than, e.g. for highway driving. We account for these differences by emissions factors derived explicitly for typical urban driving conditions for each country, with vehicle category and

Table 1. Primary NO_2 emission shares in the literature. (a) Sjödin and Jerksjö (2008); (b) Grice et al. (2009); (c) HBEFA 3.1 (2010); (d) Carslaw and Rhys-Tyler (2013); (e) Weiss et al. (2011). (c) is used in GAINS.

control	(a)	(b)	(c)	(d)	(e)
no	14 %	11 %	8 %	15 %	
Euro 1	14 %	11 %	8 %	14 %	
Euro 2	14 %	11 %	11 %	9 %	
Euro 3	47 %	30 %	28 %	16 %	
Euro 4	55 %	55 %	47 %	28 %	40 %
Euro 5	55 %	55 %	36 %	25 %	46 %
Euro 6			30 %		

technology taken from COPERT (Ntziachristos et al., 2009). Urban traffic emission trends are applied in the traffic increment calculation, and for the urban increment calculation at stations located inside urban areas.

As described in Sect. 2.3.1, the share of NO_x emitted as primary NO_2 (p in Eq. 9) is of particular importance for the calculation of roadside NO_2 concentrations. Measurements of p for different emission control technologies have been reported e.g. by Carslaw and Rhys-Tyler (2013); Sjödin and Jerksjö (2008); Weiss et al. (2011); however, significant differences are present between values for the same vehicle technology (see Table 1). In the GAINS model, p shares from the Handbook Emission Factors for road transport (HBEFA v3.1, http://www.hbefa.net) are used, which are based on chassis dynamometer tests over various driving cycles (Hausberger et al., 2009). There are no indications that this share differs between driving conditions. Therefore the same shares are used for both national and urban driving.

3 Validation: explaining historical NO_2 trends

Validating a model designed to provide results for more than 1950 individual monitoring stations across Europe poses a considerable challenge. Here we show a validation of the background modelling in the base year for all background stations on the one hand, and a validation of trends of the station-based model results on the other hand.

As a validation of calculated (explained) NO_2 urban background, Fig. 6 shows a comparison of annual mean modelled vs. observed NO_2 concentrations in the base year, at all urban background stations covered by the model. The difference between observations and modelled values constitutes the unexplained (or over-explained) component which is corrected in the scenario analysis for individual stations. Urban background stations are split up into those located inside a known urban polygon (panel a) and those for which no urban polygon is defined (panel b). While both categories show a reasonably good linear relation between observations and model calculations, the bias between model and observations

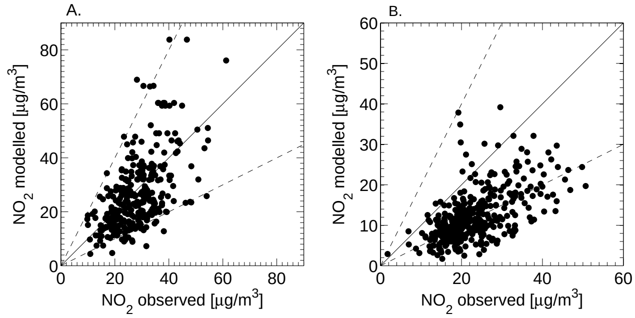

Fig. 6. Comparison of modelled (explained) vs. observed NO_2 urban background concentrations: **(A)** urban background stations in cities for which an urban polygon is defined, **(B)** urban background stations in cities for which no urban polygon is defined (7 × 7 km grid value is taken here).

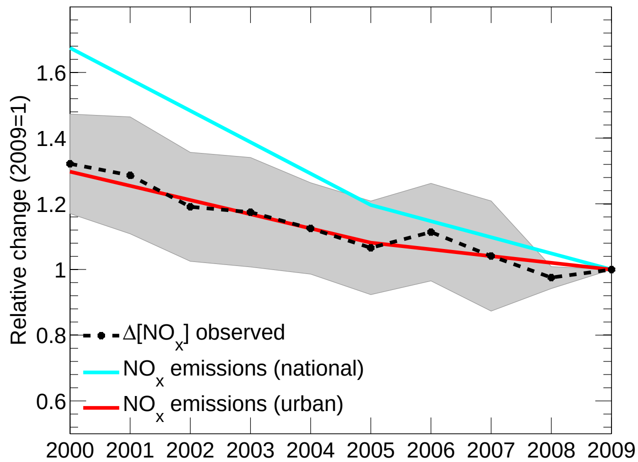

Fig. 7. Trends in observed NO_x roadside increments (black), compared to calculated emission trends for national average (blue) and urban (red) driving conditions, in Germany. All trends are shown relative to the year 2009. The spread in observations (standard deviation of the mean) is indicated as grey shaded area. Note that observations are available for every year, while emissions are calculated only in five-year intervals and interpolated linearly in between.

is lower for urban background stations within defined urban polygons. This highlights the added value of the last downscaling step beyond the 7 × 7 km resolution within cities, which becomes even more important for smaller cities. For practical reasons, a lower limit of 100 000 inhabitants was used when calculating urban polygon shapes from population density maps, leading to the underestimation of urban background concentrations in cities falling below this limit (panel b).

The ability of the parametrised traffic station model to reproduce well the observed strong variations in NO_2 concentrations in the base year is demonstrated exemplarily in Fig. 5a, with similarly strong agreement also observed at most other traffic stations.

For years other than the base year, the NO_x traffic increment is scaled with the trend in urban NO_x traffic emissions. This relation is shown in Figure 7 for Germany: here the trend in observed NO_x roadside concentration increments is compared to the trend in NO_x road traffic emissions, using either national average or urban driving conditions. The observed values contain all roadside stations with a NO_x increment $>15\,\mu g\,m^{-3}$ in 2009 and observations available for at least nine out of the ten years 2000–2009. The spread of trends measured at individual stations is indicated as shaded area (standard deviation of the mean). Observed trends in NO_x traffic increments are captured perfectly by the calculated NO_x emission trends, however, only if urban driving conditions are employed. Similarly good agreement is found in other countries with sufficiently large numbers of traffic stations to allow for a good statistical sample (in particular, France, Austria and the UK).

Figure 8 shows the trend of NO_2 and NO_x concentrations measured and modelled at all roadside monitoring stations in the EU. Only stations with monitoring data available for at least nine out of the ten years are selected. The traffic station model reproduces both trends almost perfectly well. While NO_x concentrations decline by around 25 %, NO_2 concentrations are stagnant. This discrepancy is related to strong increases in primary NO_2 emissions (Fig. 10, panel b) due to increased use of diesel vehicles, offsetting the effect of NO_x emission reductions.

Further distinguishing into Member States, Fig. 9 shows for all EU Member States with sufficient data absolute NO_2 concentrations averaged by station category (rural background, urban background, and roadside stations) for the period 2000–2009. Since the model is calibrated to monitoring data in 2009, consistency between observations and model calculations is inherently forced in this year; the other years, however, are independent of observations. To improve consistency in the observational record, only stations with more than five years of data available in the ten year period have been selected, and only countries with at least three such traffic stations are shown in Fig. 9. The same set of stations is used here for both observations and model results. Trends are in general well reproduced for all station types, especially in Austria, Germany, Netherlands, France, Sweden, and some other countries. In some countries (notably Belgium, Italy, Portugal, UK) modelled trends at traffic stations are more optimistic than observations show. A potential reason for this behaviour is the strong increase of the share of primary NO_2 in road traffic NO_x emissions (p in Eq. 9) in these countries, which is taken into account in the street canyon module but not for the urban background: in the same countries modelled urban background NO_2 concentrations also decline too fast. This is further discussed in Sect. 4.

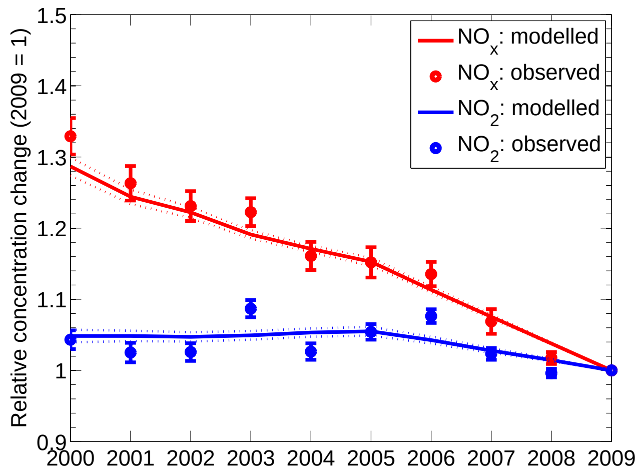

Fig. 8. Trends in NO_2 and NO_x concentrations measured and modelled at AirBase traffic stations, averaged for the whole EU. Only stations covering at least 9 out of the 10 yr are included. Concentrations are normalised to the year 2009. Standard deviations of the mean are shown as error bars for the observations and as dotted lines around modelled values.

4 Uncertainties and robust solutions

Owing to the scope of the model linking European-scale emission calculations with impacts in individual street canyons, simplifications are taken that induce uncertainty.

A systematic source of uncertainty stems from the assumptions on urban background NO_2. In the absence of reliable predictions regarding the evolution of future urban background O_3 levels, these are assumed to remain constant. Furthermore, it is assumed that urban background stations and the air masses they represent are sufficiently remote from traffic emissions to ensure that the partitioning of NO_2 and NO in urban background NO_x is determined by ambient O_3 rather than the initial share of NO_2 in traffic emissions (p). Under these assumptions, urban background NO_2 follows the same trend as urban background NO_x. In reality, this is not completely fulfilled (see e.g. Keuken et al., 2009), and urban background NO_2 declined more slowly than NO_x, especially in countries with a strong increase in the share of primary NO_2 in NO_x emissions. Altogether, this results in backward calculated urban background NO_2 in the year 2000 over-estimating observations by $\sim 2\,\mu g\,m^{-3}$ on the European average. However, the influence of the background trend on modelled roadside concentrations is limited, as the traffic increment calculation does take into account p variations. From GAINS calculations (Fig. 10b) as well as recent observations (Carslaw and Rhys-Tyler, 2013) the increases of p are expected to slow down in the future, further decreasing the relevance of this systematic deviation.

The NO_2/NO_x emission shares used in the model are subject to considerable uncertainty (see Table 1). However, errors in p are partially compensated by the parameter

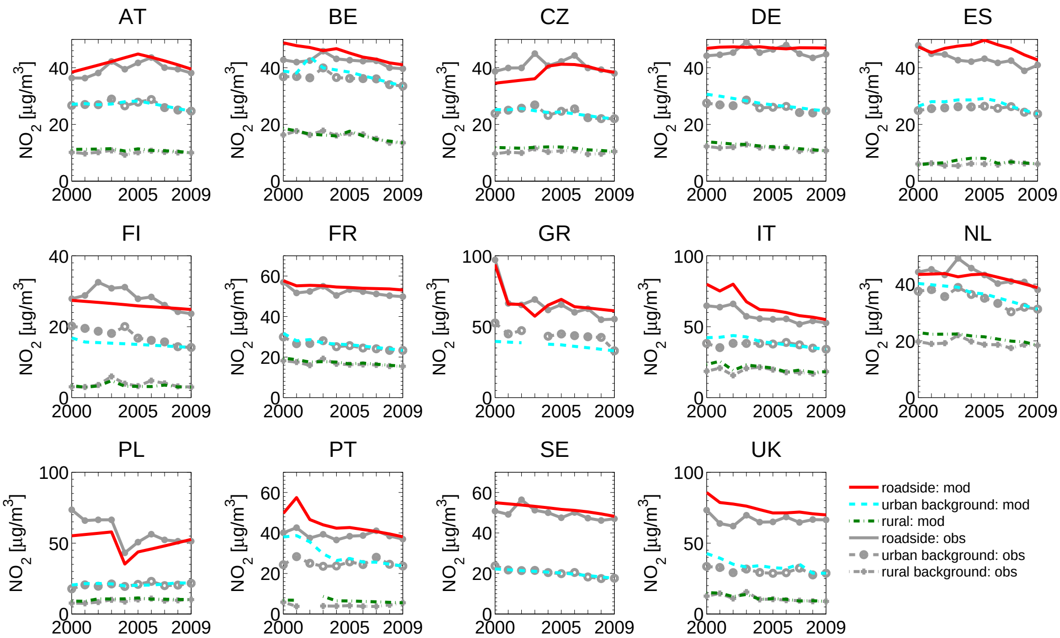

Fig. 9. Annual mean country average NO_2 concentrations modelled at different categories of AirBase monitoring stations in 14 EU Member States (coloured lines), compared to the observed values (grey lines).

estimation process, which demands that the base year observations are approximately reproduced by the model.

Other factors of uncertainty may be systematic for a single station, but may be expected to compensate in a larger ensemble of stations:

– *Selection of base year.* While the regional background calculations use a five-year average of transfer coefficients to compensate for inter-annual variability in large-scale meteorology, urban and roadside increment calculations are entirely based on model calculations and monitoring data from the year 2009. 2009 was selected as base year as this was the most recent year for which all necessary data – emission inventory, meteorological fields, and AirBase observations – were available at the starting time of this project. On the European average, there are years in the 2000–2008 period with measured concentrations above as well as below the calculations based on 2009 data, indicating that on average 2009 does not seem to be exceptional in meteorological terms. Besides meteorological factors, other local conditions such as nearby construction sites, road blocks (affecting traffic conditions and hence emissions in that area) etc. may decrease the suitability of 2009 as the base year. Given the number of stations involved, it is infeasible to check local conditions for every station; instead we have to accept unfavourable choices in individual stations.

– *Errors in observations or meta information.* The direct involvement of observations can be both beneficial and detrimental to the quality of the analysis, as it induces a strong dependency on the quality of monitoring data and station meta-information supplied by AirBase. Apart from measurement uncertainties, the positioning and classification of stations into traffic or background stations is crucial in our scheme for the disaggregation of observed concentrations into urban background and roadside increment, and the identification of the unexplained component.

– *National emission trends.* Emission trends are calculated on a national basis using national total or urban fleet compositions and average emission factors under average national or urban driving conditions. The same is true for the share of NO_2 in NO_x emissions. However, it is known from detailed analyses that traffic composition and emissions can vary significantly between stations in the same city or region.

From these considerations, it is obvious that results for individual stations have to be used with caution. Rather than actual site-specific predictions, they illustrate the likely evolution of pollution levels if local conditions are well in line with national average trend assumptions, and if no additional local measures are taken. In practice, the influence of local action or inaction may well dominate the actual resulting trend. It is not attempted to model these influences here, but rather to quantify the concentration changes that may be expected from European-wide emission control efforts, and quantify the complementary need for additional local action for achieving compliance.

As a way to deal with the random uncertainties connected with predictions for individual stations, a statistical evaluation of results is optimal. One way to do this is illustrated in Fig. 9, showing country-wide averages of concentrations for different station categories. For compliance estimates, however, the important information is the concentration at each site compared to the limit value. Therefore we analyse stations aggregated into compliance classes according to their modelled concentrations.

5 Application to the future: attainment of NO_2 limit values under current legislation

Applying the modelling scheme introduced in this article, we here assess the evolution of (possible) compliance with NO_2 limit values until 2030, assuming that only currently approved legislation is successfully implemented. This emission scenario has been used as the baseline scenario in the ongoing revision of the EU Thematic Strategy on Air Pollution.

Section 5.1 provides a short description of the assumptions taken for the generation of the emission scenario. With road traffic being the most important source of NO_x emissions for monitoring stations exceeding the limit value, the scenario description here is limited to road traffic. A discussion of other sectors, such as industrial emissions, can be found in Amann et al. (2013). The projected evolution of the compliance situation under this emission scenario is discussed in Sect. 5.2.

5.1 Trend scenario for NO_x emissions from road transport

The prospective NO_x emissions under trend assumptions are calculated in five-year steps from 2000 to 2030 combining the following elements:

- Transport and consequent fuel demand by vehicle category, based on the latest PRIMES scenario for the European Union (Amann et al., 2013),
- composition of the future vehicle fleet, based on the regular turnover and the gradual penetration of new vehicle emission control technologies (Euro 5 and Euro 6),
- mean NO_x and NO_2 emission factors for average national and urban driving conditions, for different emission control technologies.

As fleet composition and unit emissions under urban driving conditions are different from the national average, we calculate emissions for both average national as well as average urban conditions. To ensure consistency with officially reported numbers, 2005 and 2010 emission inventories have been calibrated to emissions reported under the Convention on Long-Range Transboundary Air Pollution[5] within 5–10 %, for each SNAP sector.

5.1.1 National trend for transport demand

The PRIMES model provides a consistent projection of supply and demand of energy in European Member States including the future transport demand by mode. We here use the latest PRIMES 2012/13 Reference scenario to project vehicle mileage and fuel demand. Particularly relevant for NO_x emissions is a projected strong growth of diesel cars and an assumed decline in the usage of gasoline cars in almost all EU Member States.

5.1.2 Fleet composition and turnover

The fleet composition for the historic years is based on results of the FLEETS project (Ntziachristos et al., 2008), which produced a consistent data set of detailed vehicle and activity information for road transport for each Member State. This data set has been further updated and reviewed in the framework of the LIFE EC4MACS project (see www.ec4macs.eu) and for this study based on input from national experts. Notably the purchase of used cars was modelled in detail in many countries (Mehlhart et al., 2011), resulting in an older fleet in these countries. The fuel consumption calculated bottom-up is calibrated with the fuel demand as projected by PRIMES, providing an internally consistent data set of fleet composition. A detailed description of the methodology is given by Ntziachristos and Kouridis (2008).

5.1.3 Emission factors for future vehicles

Euro 5 and Euro 6 diesel cars are particularly relevant for future NO_x emissions. Real-life emission factors for Euro 5 diesel cars and light trucks are based on recent measurements indicating higher NO_x emissions than those of Euro 4 and Euro 3 cars, exceeding the limit value defined for type approval several times (Hausberger, 2010). This analysis employs a national average value of about 870 mg NO_x/ km, i.e. almost five times higher than the nominal limit value. While the performance of Euro 6 cars under real-world driving conditions is uncertain, we assume here (optimistically) that real-world driving emissions will indeed decline in two phases: a first generation of Euro 6.1 vehicle is assumed to emit about 380 mg NO_x/ km, i.e. decreasing Euro 5 emissions by the ratio of Euro 6 to Euro 5 limit values. It is further assumed that for a second generation of Euro 6.2 vehicles the type approval testing will be complemented by, e.g. onboard portable emission measurement systems or random cycle tests. As a consequence, new vehicle types from 2017 onwards are assumed to emit 120 mg NO_x/km under real-world driving. Early demonstration vehicles have shown that selective catalytic reduction (SCR) technology with injection of

[5]Emissions available from http://www.ceip.at.

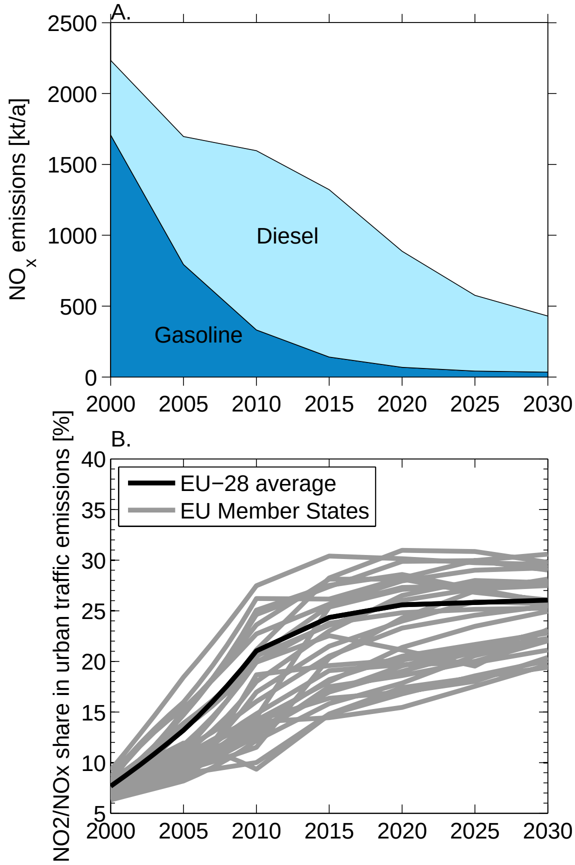

Fig. 10. (A) Trends in NO_x emissions from passenger cars in the EU-28 under the current legislation scenario. **(B)** Share of primary NO_2 in NO_x emissions from road traffic, in the individual EU Member States (grey) and the EU-28 mean (black).

appropriate amounts of urea could deliver large reductions in NO_x emissions over Euro 5 vehicles, both for type-approval and real-world cycles (Demuynck et al., 2012; Weiss et al., 2012).

5.1.4 Baseline trends for NO_x emissions

NO_x emissions from gasoline cars are expected to decrease quickly, respectively amounting in 2020 and 2030 to only 20 % and 10 % of the 2010 levels. Comparable reductions are expected from heavy duty trucks and diesel buses. NO_x emissions from diesel cars start declining later and decline more slowly, respectively reaching 65 % and 31 % of 2010 values in 2020 and 2030. NO_x emission trends of passenger cars are shown in Fig. 10a. While total NO_x emissions from road transport decrease, the fraction of NO_x emitted as NO_2 increases further, however, gradually levelling off at an average of 25 % (Fig. 10b).

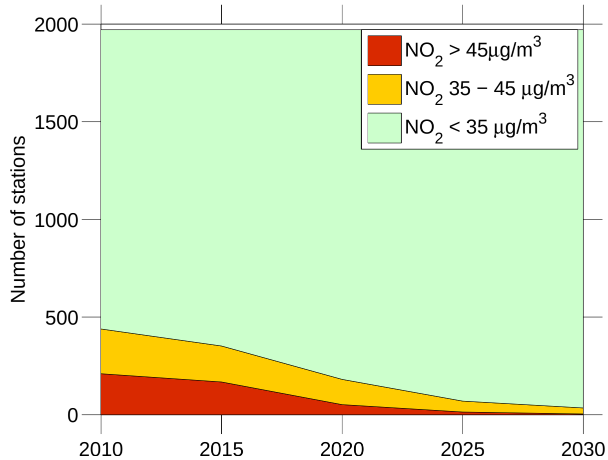

Fig. 11. Projected NO_2 compliance under current legislation: numbers of stations in the different compliance categories, EU-28 total.

5.2 Results: attainment of air quality limit values

Figure 11 shows the modelled evolution of NO_2 concentrations in the EU-28. To reflect unavoidable uncertainties in monitoring data, modelling techniques and future meteorological conditions as discussed in Sect. 4, results are expressed as numbers of stations aggregated in different "compliance categories": annual mean NO_2 concentrations below 35 $\mu g\,m^{-3}$ (i.e. at least 5 $\mu g\,m^{-3}$ below the limit value) indicate rather likely attainment of the limit value (shaded in green). For concentrations computed between 35 and 45 $\mu g\,m^{-3}$ (shaded in yellow), attainment is possible but uncertain due to the factors mentioned above. Stations with modelled concentrations higher than 45 $\mu g\,m^{-3}$ (shaded in red) are unlikely to attain the limit value. The $\pm 5\,\mu g\,m^{-3}$ range was chosen as it corresponds to the maximum deviation between modelled and observed NO_2 at the European average of all traffic stations in any of the years 2000–2008. It does not reflect a defined level of likelihood in the mathematical sense. The set of stations considers only those modelled in the base year; as new monitoring stations are put into operation, the absolute numbers may change in the future.

The projected decline in NO_x emissions should significantly improve future compliance with NO_2 air quality limit values, decreasing the number of stations severely exceeding the limit value ($NO_2 > 45\,\mu g\,m^{-3}$) by a factor of four by 2020 in the EU-28; by 2030, if Euro 6 vehicle emission standards work as effectively as assumed here, almost all cases of severe non-compliance should be eliminated. However, by 2030 around 30 stations are still projected to remain in the "attainment uncertain" category, for which reliable conclusions about attainment are impossible due to uncertainties in the modelling scheme as discussed in Sect. 4.

To illustrate the strong geographical contrasts, a map of the spatial distribution of stations in different compliance categories is shown in Fig. 12 for the year 2020. Difficulties in

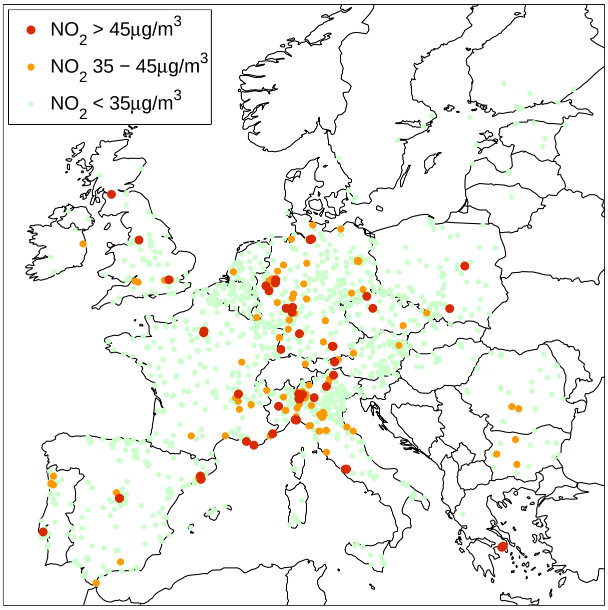

Fig. 12. Map of stations in different compliance categories as projected for 2020 under current legislation.

achieving compliance are expected to remain for many of the major European cities, such as London, Paris, Rome, Madrid, Milan, the Ruhr area or Athens. Since these major cities are home to a significant proportion of the European population, the few stations exceeding the limit value by 2025 or even 2030 have disproportionally larger implications on possible population exposure than their small absolute number in Fig. 11 would suggest.

As discussed in Sect. 4, a fundamental assumption behind the projected concentrations is that emission trends at each station follow the national average (for urban conditions if applicable). Local measures, be they beneficial or detrimental, are not modelled, though they may have a major impact on resulting concentrations. In particular, additional local action may be required to ensure attainment of the limit value at the remaining critical stations.

6 Conclusions

This paper presents an introduction to the downscaling methodology that has been implemented in the GAINS integrated assessment model for estimating compliance with air quality limit values. Employing a chain of models of different scales, we link European-wide emission control policies with impacts in street canyons.

Results are calculated for more than 400 roadside and around 1550 background monitoring stations reporting to AirBase, including 70 % of the stations exceeding the NO_2 limit value in 2009. Station-specific characteristics of roadside stations are reflected in the parameters estimated from past observations. In the absence of more detailed information for individual stations, emission trends are taken from national calculations, enabling us to analyse station ensembles rather than individual stations. On the other hand, the scheme may as well be applied to model individual stations if localised emission data become available.

The model reproduces well the observed trends in the decade 2000–2009. NO_2 concentrations were relatively stagnant in this decade, especially at urban traffic hot spots, in spite of declining NO_x emissions. This is explained by strong increases in the share of primary NO_2 emissions, predominantly due to increasing shares of diesel cars in European fleets.

In spite of the stagnant NO_2 levels in the past, the model projects declining NO_2 concentrations in the future, if currently approved legislation is successfully implemented. The main reason behind the expected change in trend is the assumption that new exhaust cleaning technologies introduced with the Euro 6 emission standard will deliver strong reductions in real-world NO_x emissions from diesel cars from 2015/2017 onwards. In general, our projections show that under the assumptions taken, Europe is on the right track towards achieving compliance with NO_2 limit values in the medium term. At some monitoring stations, however, safe attainment of limit values is not even foreseen until 2030, pointing to the need for additional European legislation or complementary local action to reduce NO_x emissions.

Appendix A

The gridded emission inventory

The gridded distribution of anthropogenic emissions used in the CTM simulations are provided by INERIS. They are based on a merging of databases from:

- TNO 0.125° × 0.0625° emissions for 2007 from MACC (Kuenen et al., 2011, see also http://www.gmes-atmosphere.eu/),
- EMEP 0.5° × 0.5° emissions for 2009, available through the EMEP Centre on Emission Inventories and Projections (CEIP; http://www.ceip.at/),
- emission data from the GAINS database,
- INERIS expertise on re-gridding with various proxies (population, land use, large point source data).

First the large point sources (LPS) from the fine-scale (0.125° × 0.0625°) TNO-MACC emissions data for 2007 were added to surface emissions to get only one type of emissions; emission heights were then ascribed in a second step using standard profiles as documented by Bieser et al. (2011). For the various activity sectors the processing steps were the following:

– SNAP 2: the country emissions were re-gridded with coefficients based on population density and French bottom-up data, the methodology was extrapolated to the whole of Europe. To give a more realistic representation of increased domestic heating emissions in winter, a temperature proxy (degree days) was used for the temporal modulation of SNAP 2 emissions.

– SNAP 3, 7, 8, 9, 10: TNO-MACC emissions were used as proxy to re-grid EMEP $0.5° \times 0.5°$ annual totals. In particular, for road traffic emissions (SNAP 7) the TNO-MACC pattern includes the major road network, and for off-road transport emissions (SNAP 8) inland waterways.

– SNAP 1, 4, 5, 6: EMEP $0.5° \times 0.5°$ emissions were re-gridded by adequate proxies ("artificial land use", EPER data for industries).

For countries where MACC-TNO emissions are not available EMEP $0.5° \times 0.5°$ emissions were used (Iceland, small countries, Asian countries). This inventory is interfaced with the CHIMERE model using chemical speciation and adequate temporal profiles. The procedure is fully documented by Menut et al. (2012).

Appendix B

Urban polygon shapes

Shapes of 473 European cities and urban agglomerations with more than 100 000 inhabitants were constructed based on population density distribution at a $0.01° \times 0.01°$ resolution which were obtained from the Institute for Environment and Sustainability, Joint Research Centre in Ispra (see Gallego, 2010).

Population numbers for cities and urban agglomerations were obtained from the www.citypopulation.de database. Information about the location of cities was taken from the Global Rural-Urban Mapping Project (GRUMP, http://sedac.ciesin.columbia.edu/data/dataset/grump-v1-settlement-points).

From the above-mentioned input data, city and agglomeration shapes were constructed using GIS. The algorithm was based on ascending sorting of grid cells according to a weighting function x,

$$x = \frac{d^2}{\sigma_{\mathrm{pop}}}, \tag{B1}$$

with d distance from city center and σ_{pop} population density in the grid cell. The cut-off for x (determining the city shapes) was based on the condition that the differences between the reported numbers of population living in each city and the population numbers calculated inside the corresponding shapes are minimised. Thus the value of the cut-off was set by the minimum of RMSE calculated for these differences.

Acknowledgements. This work was partially supported by the EC4MACS (European Consortium for the Modelling of Air pollution and Climate Strategies) project with the contribution of the LIFE financial instrument of the European Community (contract no. LIFE06 ENV/PREP/A/000006), as well as the Service Contract on Monitoring and Assessment of Sectorial Implementation Actions (contract no. 07.0307/2011/599257/SER/C3) of DG-Environment of the European Commission. The authors would like to thank H. Fagerli and A. Nyiri (MSC-W) for conducting the EMEP model simulations underlying the 28 km transfer coefficients. Monitoring data used in this study were obtained from AirBase (version 5).

Edited by: R. Harley

References

Amann, M., Bertok, I., Borken-Kleefeld, J., Cofala, J., Heyes, C., Höglund-Isaksson, L., Klimont, Z., Nguyen, B., Posch, M., Rafaj, P., Sandler, R., Schöpp, W., Wagner, F., and Winiwarter, W.: Cost-effective control of air quality and greenhouse gases in Europe: Modeling and policy applications, Environ. Modell. Softw., 26, 1489–1501, doi:10.1016/j.envsoft.2011.07.012, 2011.

Amann, M., Borken-Kleefeld, J., Cofala, J., Hettelingh, J.-P., Heyes, C., Holland, M., Kiesewetter, G., Klimont, Z., Rafaj, P., Paasonen, P., Posch, M., Sander, R., Schoepp, W., Wagner, F., and Winiwarter, W.: Policy Scenarios for the Revision of the Thematic Strategy on Air Pollution. TSAP Report #10, International Institute for Applied Systems Analysis (IIASA), Laxenburg, Austria, 2013.

Berkowicz, R.: OSPM – A Parameterised Street Pollution Model, Environ. Monit. Assess., 65, 323–331, 2000.

Bessagnet, B., Menut, L., Curd, G., Hodzic, A., Guillaume, B., Liousse, C., Moukhtar, S., Pun, B., Seigneur, C., and Schulz, M.: Regional modeling of carbonaceous aerosols over Europe-focus on secondary organic aerosols, J. Atmos. Chem., 61, 175–202, doi:10.1007/s10874-009-9129-2, 2008.

Bieser, J., Aulinger, A., Matthias, V., Quante, M., and van der Gon, H. D.: Vertical emission profiles for Europe based on plume rise calculations, Environ. Pollut., 159, 2935–2946, doi:10.1016/j.envpol.2011.04.030, 2011.

Campling, P., Janssen, L., Vanherle, K., Cofala, J., Heyes, C., and Sander, R.: Specific evaluation of emissions from shipping including assessment for the establishment of possible new emission control areas in European Seas. Final Report., Flemish Institute for Technological Research (VITO), Mol, BE, 2013.

Carslaw, D. C.: Evidence of an increasing NO_2/NO_X emissions ratio from road traffic emissions, Atmos. Environ., 39, 4793–4802, doi:10.1016/j.atmosenv.2005.06.023, 2005.

Carslaw, D. C. and Rhys-Tyler, G.: New insights from comprehensive on-road measurements of NO_x, NO_2 and NH_3 from vehicle emission remote sensing in London, UK, Atmos. Environ., 81, 339–347, doi:10.1016/j.atmosenv.2013.09.026, 2013.

Carslaw, D., Beevers, S., Westmoreland, E., Williams, M., Tate, J., Murrells, T., Stedman, J., Li, Y., Grice, S., Kent, A., and Tsagatakis, I.: Trends in NO_x and NO_2 emissions and ambient measurements in the UK, Report prepared for Defra, UK, http://uk-air.defra.gov.uk/reports/cat05/1108251149_110718_AQ0724_Final_report.pdf, 2011a.

Carslaw, D. C., Beevers, S. D., Tate, J. E., Westmoreland, E. J., and Williams, M. L.: Recent evidence concerning higher NO_x emissions from passenger cars and light duty vehicles, Atmos. Environ., 45, 7053–7063, doi:10.1016/j.atmosenv.2011.09.063, 2011b.

Cyrys, J., Eeftens, M., Heinrich, J., Ampe, C., Armengaud, A., Beelen, R., Bellander, T., Beregszaszi, T., Birk, M., Cesaroni, G., Cirach, M., de Hoogh, K., Nazelle, A. D., de Vocht, F., Declercq, C., Dėdelė, A., Dimakopoulou, K., Eriksen, K., Galassi, C., Graulevičienė, R., Grivas, G., Gruzieva, O., Gustafsson, A. H., Hoffmann, B., Iakovides, M., Ineichen, A., Krämer, U., Lanki, T., Lozano, P., Madsen, C., Meliefste, K., Modig, L., Mölter, A., Mosler, G., Nieuwenhuijsen, M., Nonnemacher, M., Oldenwening, M., Peters, A., Pontet, S., Probst-Hensch, N., Quass, U., Raaschou-Nielsen, O., Ranzi, A., Sugiri, D., Stephanou, E. G., Taimisto, P., Tsai, M.-Y., Éva Vaskövi, Villani, S., Wang, M., Brunekreef, B., and Hoek, G.: Variation of NO_2 and NO_x concentrations between and within 36 European study areas: Results from the ESCAPE study, Atmos. Environ., 62, 374–390, doi:10.1016/j.atmosenv.2012.07.080, 2012.

Demuynck, J., Bosteels, D., Paepe, M. D., Favre, C., May, J., and Verhelst, S.: Recommendations for the new WLTP cycle based on an analysis of vehicle emission measurements on NEDC and CADC, Energ. Policy, 49, 234–242, doi:10.1016/j.enpol.2012.05.081, 2012.

Denby, B. R.: Guide on modelling Nitrogen Dioxide (NO_2) for air quality assessment and planning relevant to the European Air Quality Directive, ETC/ACM Technical Paper 2011/15. European Topic Centre on Air Pollution and Climate Change Mitigation, 2011.

Dilks, D. W., Canale, R. P., and Meier, P. G.: Development of Bayesian Monte Carlo techniques for water quality model uncertainty, Ecol. Model., 62, 149–162, 1992.

Düring, I., Bächlin, W., Ketzel, M., Baum, A., Friedrich, U., and Wurzler, S.: A new simplified NO/NO_2 conversion model under consideration of direct NO_2-emissions, Meteorol. Z., 20, 67–73, doi:10.1127/0941-2948/2011/0491, 2011.

EEA: EMEP/CORINAIR Emission Inventory Guidebook – 2007, Technical Report No. 16/2007. European Environment Agency, Copenhagen, DK, http://www.eea.europa.eu/publications/EMEPCORINAIR5 (last access: 21 January 2014), 2007.

EEA: Air quality in Europe – 2012 report, Report No. 4/2012, European Environment Agency, Copenhagen, DK, 2012.

EU: Directive 2008/50/EC of the European Parliament and of the Council of 21 May 2008 on ambient air quality and cleaner air for Europe (Offic J EU, L 152, 11 June 2008, 1–44), 2008.

Gallego, F. J.: A population density grid of the European Union, Popul. Environ., 31, 460–473, doi:10.1007/s11111-010-0108-y, 2010.

Grice, S., Stedman, J., Kent, A., Hobson, M., Norris, J., Abbott, J., and Cooke, S.: Recent trends and projections of primary NO2 emissions in Europe, Atmos. Environ., 43, 2154–2167, doi:10.1016/j.atmosenv.2009.01.019, 2009.

Hausberger, S.: Fuel consumption and emissions of modern passenger cars, Report No. I-25/10, Institute for Internal Combustion Engines and Thermodynamics, Graz University of Technology, Graz, Austria, 2010.

Hausberger, S., Rexeis, M., Zallinger, M., and Luz, R.: Emission Factors from the Model PHEM for the HBEFA Version 3, Report Nr. I-20/2009 Haus-Em 33/08/679 from 07 December 2009, Institute for Internal Combustion Engines and Thermodynamics, Graz University of Technology, Graz, Austria, http://www.hbefa.net/d/documents/HBEFA_31_Docu_hot_emissionfactors_PC_LCV_HDV.pdf, 2009.

Keuken, M., Roemer, M., and van den Elshout, S.: Trend analysis of urban NO_2 concentrations and the importance of direct NO_2 emissions versus ozone/NO_x equilibrium, Atmos. Environ., 43, 4780–4783, doi:10.1016/j.atmosenv.2008.07.043, 2009.

Knoerr, W., Duennebeil, F., Lambrecht, U., and Schacht, A.: Aktualisierung "Daten- und Rechenmodell: Energieverbrauch und Schadstoffemissionen des motorisierten Verkehrs in Deutschland 1960–2030" (TREMOD, Version 5.3) für die Emissionsberichtserstattung 2013 (Berichtsperiode 1990–2011), Endbericht, ifeu Institut, Heidelberg, Germany, 2012.

Kuenen, J., Denier van der Gon, H., Visschedijk, A., Van der Brugh, H., and Gijlswijk, R.: MACC European emission inventory for the years 2003–2007, TNO-report TNO-060-UT-2011-00588, Utrecht, 2011.

Mehlhart, G., Mertz, C., Akkermans, L., and Jordal-Jørgensen, J.: European second-hand car market analysis. Final Report, Öko-Institut, Darmstadt, Germany, 2011.

Menut, L., Goussebaile, A., Bessagnet, B., Khvorostiyanov, D., and Ung, A.: Impact of realistic hourly emissions profiles on air pollutants concentrations modelled with CHIMERE, Atmos. Environ., 49, 233–244, doi:10.1016/j.atmosenv.2011.11.057, 2012.

Menut, L., Bessagnet, B., Khvorostyanov, D., Beekmann, M., Blond, N., Colette, A., Coll, I., Curci, G., Foret, G., Hodzic, A., Mailler, S., Meleux, F., Monge, J.-L., Pison, I., Siour, G., Turquety, S., Valari, M., Vautard, R., and Vivanco, M. G.: CHIMERE 2013: a model for regional atmospheric composition modelling, Geosci. Model Dev., 6, 981–1028, doi:10.5194/gmd-6-981-2013, 2013.

Miglietta, M. M., Thunis, P., Georgieva, E., Pederzoli, A., Bessagnet, B., Terrenoire, E., and Colette, A.: Evaluation of WRF model performance in different European regions with the DELTA-FAIRMODE evaluation tool, Int. J. Environ. Pollut., 50, 83–97, 2012.

Murena, F., Favale, G., Vardoulakis, S., and Solazzo, E.: Modelling dispersion of traffic pollution in a deep street canyon: Application of CFD and operational models, Atmos. Environ., 43, 2303–2311, doi:10.1016/j.atmosenv.2009.01.038, 2009.

Ntziachristos, L. and Kouridis, C.: The TREMOVE/COPERT transport models, A LIFE+ EC4MACS report. Laboratory of Applied Thermodynamics, Aristotle University Thessaloniki, available at: http://www.ec4macs.eu/content/report/EC4MACS_Publications/MR_Final%20in%20pdf/TREMOVE_Methodologies_Final.pdf (last access: 21 January 2014), 2012.

Ntziachristos, L., Mellios, G., Kouridis, C., Papageorgiou, T., Theodosopoulou, M., Samaras, Z., Zierock, K.-H., Kouvaritakis, N., Panos, E., Karkatsoulis, P., Schilling, S., Meretei, T., Bodor, P., Damjanovic, S., and Petit, A.: European Database of Vehicle Stock for the Calculation and Forecast of Pollutant and Greenhouse Gases Emissions with TREMOVE and COPERT, LAT Report No: 08.RE.0009.V2. Laboratory of Applied Thermodynamics (LAT), Thessaloniki, Greece, 2008.

Ntziachristos, L., Gkatzoflias, D., Kouridis, C., and Samaras, Z.: COPERT: A European Road Transport Emission Inventory Model., in: Information Technologies in Environmental Engineering – Proceedings of the 4th International ICSC Symposium Thessaloniki, Greece, 28–29 May 2009, 491–504, Springer Berlin Heidelberg, 2009.

Palmgren, F., Berkowicz, R., Hertel, O., and Vignati, E.: Effects of reduction of NO_x on the NO_2 levels in urban streets, Sci. Total Environ., 189–190, 409–415, 1996.

Sabatino, S. D., Buccolieri, R., Pulvirenti, B., and Britter, R.: Simulations of pollutant dispersion within idealised urban-type geometries with CFD and integral models, Atmos. Environ., 41, 8316–8329, doi:10.1016/j.atmosenv.2007.06.052, 2007.

Schmidt, H., Derognat, C., Vautard, R., and Beekmann, M.: A comparison of simulated and observed ozone mixing ratios for the summer of 1998 in Western Europe, Atmos. Environ., 35, 6277–6297, doi:10.1016/S1352-2310(01)00451-4, 2001.

Simpson, D., Benedictow, A., Berge, H., Bergström, R., Emberson, L. D., Fagerli, H., Flechard, C. R., Hayman, G. D., Gauss, M., Jonson, J. E., Jenkin, M. E., Nyíri, A., Richter, C., Semeena, V. S., Tsyro, S., Tuovinen, J.-P., Valdebenito, Á., and Wind, P.: The EMEP MSC-W chemical transport model – technical description, Atmos. Chem. Phys., 12, 7825–7865, doi:10.5194/acp-12-7825-2012, 2012.

Sjödin, A. and Jerksjö, M.: Evaluation of European road transport emission models against on-road emission data as measured by optical remote sensing, in: Proceedings of the 17th International Transport and Air Pollution Conference, Graz, Austria, 2008.

Solazzo, E., Cai, X., and Vardoulakis, S.: Improved parameterisation for the numerical modelling of air pollution within an urban street canyon, Environ. Modell. Softw., 24, 381–388, 2009.

Vardoulakis, S., Fisher, B. E., Pericleous, K., and Gonzalez-Flesca, N.: Modelling air quality in street canyons: a review, Atmos. Environ., 37, 155–182, doi:10.1016/S1352-2310(02)00857-9, 2003.

Vautard, R., Honoré, C., Beekmann, M., and Rouil, L.: Simulation of ozone during the August 2003 heat wave and emission control scenarios, Atmos. Environ., 39, 2957–2967, doi:10.1016/j.atmosenv.2005.01.039, 2005.

Weiss, M., Bonnel, P., Hummel, R., Provenza, A., and Manfredi, U.: On-Road Emissions of Light-Duty Vehicles in Europe, Environ. Sci. Technol., 45, 8575–8581, doi:10.1021/es2008424, 2011.

Weiss, M., Bonnel, P., Kühlwein, J., Provenza, A., Lambrecht, U., Alessandrini, S., Carriero, M., Colombo, R., Forni, F., Lanappe, G., Lijour, P. L., Manfredi, U., Montigny, F., and Sculati, M.: Will Euro 6 reduce the NO_x emissions of new diesel cars? – Insights from on-road tests with Portable Emissions Measurement Systems (PEMS), Atmos. Environ., 62, 657–665, doi:10.1016/j.atmosenv.2012.08.056, 2012.

WHO: Air quality guidelines – global update 2005, World Health Organization Regional Office for Europe, Copenhagen, DK, 2006.